

Heterojunction photodiode fabricated from multiwalled carbon nanotube/ZnO nanowire/p-silicon composite structure

Dali Shao, Mingpeng Yu, Jie Lian, and Shayla Sawyer

Citation: *Appl. Phys. Lett.* **102**, 021107 (2013); doi: 10.1063/1.4776691

View online: <http://dx.doi.org/10.1063/1.4776691>

View Table of Contents: <http://apl.aip.org/resource/1/APPLAB/v102/i2>

Published by the [American Institute of Physics](http://www.aip.org).

Related Articles

Study of bandwidth enhancement and non-linear behavior in avalanche photodiodes under high power condition
J. Appl. Phys. **113**, 044509 (2013)

Two-photon-absorption photodiodes in Si photonic-crystal slow-light waveguides
Appl. Phys. Lett. **102**, 031114 (2013)

Near-infrared photodetection of β -FeSi₂/Si heterojunction photodiodes at low temperatures
Appl. Phys. Lett. **102**, 032107 (2013)

Silicon sub-bandgap photon linear detection in two-photon experiments: A photo-assisted Shockley-Read-Hall mechanism
Appl. Phys. Lett. **102**, 031105 (2013)

High responsivity of amorphous indium gallium zinc oxide phototransistor with Ta₂O₅ gate dielectric
Appl. Phys. Lett. **101**, 261112 (2012)

Additional information on *Appl. Phys. Lett.*

Journal Homepage: <http://apl.aip.org/>

Journal Information: http://apl.aip.org/about/about_the_journal

Top downloads: http://apl.aip.org/features/most_downloaded

Information for Authors: <http://apl.aip.org/authors>

ADVERTISEMENT

AIP | Applied Physics
Letters

SURFACES AND INTERFACES
Focusing on physical, chemical, biological, structural, optical, magnetic and electrical properties of surfaces and interfaces, and more...

ENERGY CONVERSION AND STORAGE
Focusing on all aspects of static and dynamic energy conversion, energy storage, photovoltaics, solar fuels, batteries, capacitors, thermoelectrics, and more...

EXPLORE WHAT'S NEW IN APL

SUBMIT YOUR PAPER NOW!

Heterojunction photodiode fabricated from multiwalled carbon nanotube/ZnO nanowire/p-silicon composite structure

Dali Shao,¹ Mingpeng Yu,^{2,3} Jie Lian,² and Shayla Sawyer¹

¹*Electrical, Computer, and Systems Engineering Department, Rensselaer Polytechnic Institute, Troy, New York 12180, USA*

²*Department of Mechanical, Aerospace & Nuclear Engineering, Rensselaer Polytechnic Institute, Troy, New York 12180, USA*

³*Department of Physics, School of Mathematics and Physics, University of Science and Technology Beijing, 30 Xueyuan Road, Haidian District, Beijing 100083, China*

(Received 11 August 2012; accepted 2 January 2013; published online 16 January 2013)

A heterojunction photodiode was fabricated from multiwalled carbon nanotubes (MWCNTs)/ZnO nanowires/p-Si (100) substrate composite structure. The heterojunction photodiode demonstrated a faster transient response and higher responsivity than the reference sample without deposition of MWCNTs, which is attributed to improved carrier collection and transport efficiency through the MWCNTs network. The high photoresponsivities of the devices are explained in terms of operation as a hybrid of photodiode and photoconductor modes. The spectral response of the devices showed dependence on voltage polarity and is attributed to the high valance band offset in the interfacial region of ZnO and p-Si substrate. © 2013 American Institute of Physics.

[<http://dx.doi.org/10.1063/1.4776691>]

As a wide band gap semiconductor material, ZnO has drawn much attention due to its unique optical and electrical properties including wide band gap (3.37 eV), large exciton binding energy 60 meV, high photoconductivity gain, and strong resistance to high energy proton irradiation.^{1,2} In particular, ZnO nanowires (NWs) are promising for optoelectronic applications including ultraviolet (UV) light-emitting diodes (LED), UV laser diodes, and UV photodetectors.^{3–5} By now, many methods have been used to synthesize ZnO NWs, including physical vapor depositions,⁶ hydrothermal methods,⁷ electrochemistry depositions,⁸ metal-organic chemical vapor depositions (MOCVD),⁹ and sol-gel synthesis methods.¹⁰ However, most obtained ZnO NWs have high density of interspaces, which reduce the quality of metal contacts and carrier collection efficiency. To fabricate highly sensitive ZnO NWs based UV photodetectors, it is essential to develop a method to improve the carrier collection efficiency without significantly adding cost or processing steps.

In this study, a heterojunction photodiode was fabricated using a multiwalled carbon nanotubes (MWCNTs)/ZnO NWs/p-Si structure. The MWCNTs network as electrode reduce the series resistance of the ZnO NWs array and therefore effectively improved carrier collection and transportation efficiency, leading a faster transient response and higher photoresponsivity compared with the reference sample without deposition of the MWCNTs network. The photoresponsivity spectra of the devices in the UV and visible regions depend on the polarity of the applied voltages, which is explained in terms of energy band structure and the carrier transportation mechanism inside the heterojunction structure.

Ammonium hydroxide (28 wt. %) was added dropwise into 0.1 M zinc chloride solution until the pH is 10–11 and the solution was clear. Subsequently, the transparent solution was transferred to a Teflon-lined autoclave (Parr, USA) and the p-Si substrate (boron, 10^{15} cm^{-3}) with ZnO nanoparticles as a seed layer was suspended in the solution at 95 °C for 3 h

in a regular laboratory oven. Then, the growth solution was cooled down to room temperature naturally. The resulting substrate was thoroughly washed with deionized water and absolute ethanol for several times and dried in air at room temperature. After the growth of ZnO NWs, MWCNTs with carboxyl functionalized group were resolved in dimethylformamide (DMF) and deposited onto the top of ZnO NWs to form MWCNTs network. Then aluminum (Al) contacts were deposited on top of the sample using E-beam evaporation through a shadow mask. The Al contacts had a thickness of about 250 nm and were patterned as interdigitated fingers. The inter-electrode distance is approximately 4 mm. Finally, the photodetector was packaged and wire bonded using Epo-Tek H20E conductive epoxy and was labeled as D1. For comparison, another heterojunction photodiode without deposition of the MWCNTs network was fabricated through the same process and was labeled as D2.

Figure 1(a) illustrates the 3 dimensional view of the photodiode. Top contacts with interdigitated patterns were used to enhance the carrier collection efficiency. The Raman spectra presented in Figure 1(b) prove the high quality of the ZnO NWs. The morphologies of the ZnO NWs before and after the deposition of MWCNTs are shown in Figures 1(c) and 1(d), respectively. Note that the average diameter and length of the ZnO NWs are about 80 nm and 650 nm, respectively. The sheet resistance of the MWCNTs network was measured using a similar MWCNTs network deposited on glass, which was determined to be 53 Ω /square.

The typical I-V characteristics of D1 and D2 were measured under dark environment and illumination by a 335 nm UV LED with intensity of 31.65 mW/cm², as shown in Figure 2. The reverse saturation current (at –3 V) of D1 and D2 was determined to be 2.1×10^{-5} A and 9×10^{-6} A, respectively. The inset of Figure 2 is the log scale of the measured photocurrent and dark current. The photocurrent to dark current ratio is about 6–9 for both devices when reverse

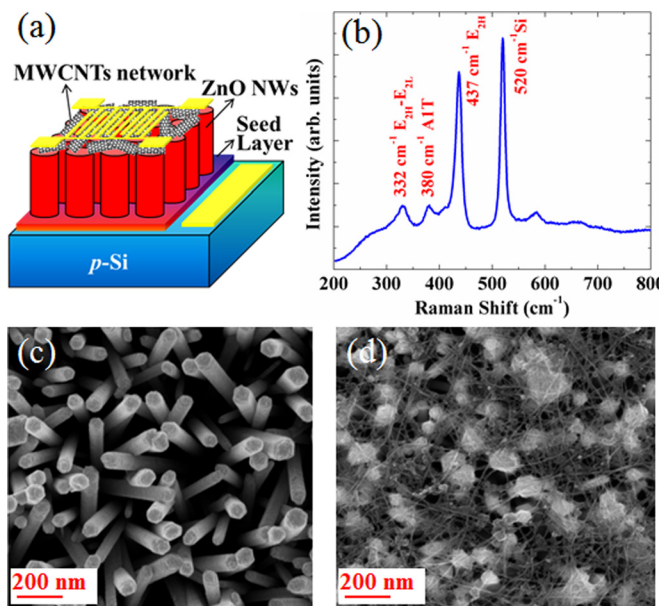


FIG. 1. (a) 3 dimensional view of heterojunction photodiode fabricated from ZnO NWs grown on top of *p*-Si substrates. (b) Raman spectra of the ZnO NWs on top of *p*-Si substrate. (c) High resolution SEM images showing the morphology of the ZnO nanowires before deposition of MWCNTs network and (d) with MWCNTs network on the top.

biased. The higher dark current and photocurrent of D1 are due to the improved conductivity by applying the MWCNTs. The dark current under forward bias increases exponentially following the equation, $I \sim \exp(\alpha V)$, which is usually observed in the wide band gap p-n diodes due to a recombination-tunneling mechanism.^{11,12} The constant α for D1 and D2 was evaluated to be 0.39 V^{-1} and 0.27 V^{-1} , respectively.

The transient response of D1 and D2 is shown in Figure 3(a), which was measured by turning on and off a 335 nm UV LED. The rise time (as measured from 10% to 90%) and fall time (from 90% to 10%) of D1 were measured to be 0.09 s and 0.08 s, respectively. This is much faster than D2, for which the rise time and fall time were measured to be 2.1 s and 1.5 s, respectively. D1 is also more than 20 times faster than other reported ZnO NWs/*p*-Si heterojunction photodiodes.^{12,13} The relative fast transient photoresponse can

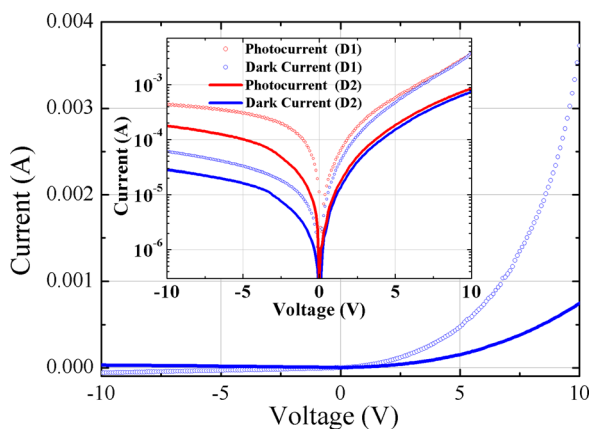


FIG. 2. I-V curve of the photodiode measured under dark environment. Inset: log scale of the I-V curve measured under dark and under UV illumination.

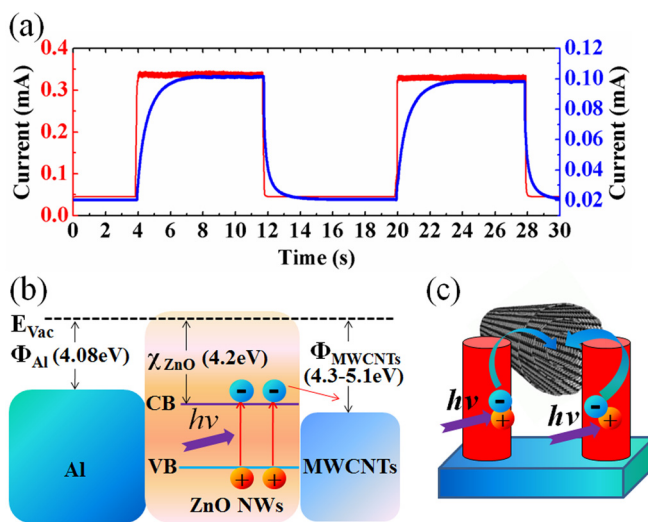


FIG. 3. (a) Transient response of D1 and D2 measured by turning on and off a 335 nm UV LED. (b) Band diagram of Al/ZnO NWs/MWCNT system. (c) Carrier transport process of the ZnO NWs/MWCNT interface.

be understood from the energy band diagram and carrier transportation process of the ZnO NWs/MWCNT interface shown in Figures 3(b) and 3(c). The electron affinity for ZnO is about 4.2 eV and the Fermi level of the MWCNT is known to be 4.3–5.1 eV below the vacuum level.^{14,15} Thus, it is energetically favorable for the electron to transfer from the ZnO to the MWCNTs when they are in contact with each other. Under UV illumination, the photogenerated electrons reach the ZnO conduction band and then transfer to the MWCNTs. Due to the semi-metallic property of the MWCNTs,¹⁶ the composite structure is expected to have better conductivity and therefore reduce the series resistance effect in the bare ZnO NWs array. This effectively enhances the electron-hole separation and improves carrier transport in the composite structure, leading to a faster rise of the photocurrent. When the UV illumination is turned off, excess electrons in the MWCNTs side transfer to the ZnO side and recombine with the holes, which is an inherently fast process.¹⁷ Note that the on/off ratio for both D1 and D2 is low (< 10), which is attributed to high dark current of the two devices. Further improvement of the transient response and the on/off ratio may be done using oxygen plasma treatment reported by Liu and Kim, which can significantly improve the time response ($50 \mu\text{s}$) and on/off ratio (~ 1000) of ZnO epitaxial films by reducing surface oxygen vacancies.¹⁸ Moreover, surface passivation using polymethyl methacrylate (PMMA) or polyvinyl-alcohol (PVA) can also effectively reduce the density of surface defects, leading lower dark current and hence higher on/off ratio.^{19–21}

The photoresponsivity spectra of the D1 and D2 under reverse and under forward bias conditions are shown in Figure 4. A maximum responsivity of 4.7 A/W for UV light (365 nm) at 2 V reverse bias was observed for D1, which is 3 times higher than that of D2. The higher photoresponsivity of D1 is attributed to the improved carrier collection and transport efficiency as a result of improved device integrity by applying MWCNTs network. Moreover, the photoresponsivities of D1 and D2 are much higher than most of the published results regarding ZnO/*p*-Si heterojunction photodiodes,^{22–27} which is

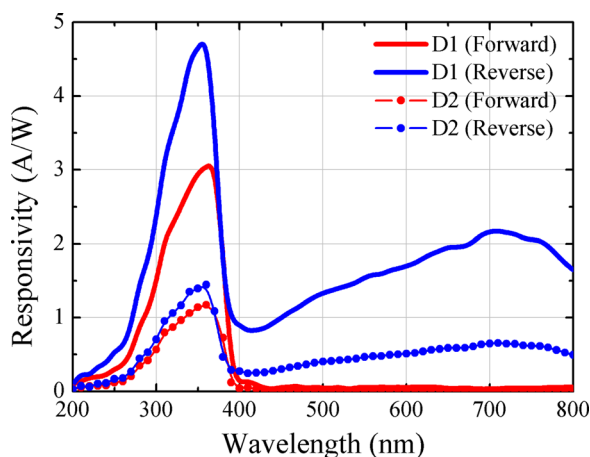


FIG. 4. Photoresponsivity spectra of the D1 and D2 measured under reverse and forward biases.

attributed to high internal gain originates from the ZnO NWs. It is widely accepted that the surface oxygen molecules adsorption and desorption process can introduce high internal gain for ZnO NWs.^{3,28} Since the ZnO NWs in this work are long (>500 nm), the longitudinal transport of photogenerated carriers would then be governed by both the depletion region of the ZnO/*p*-Si junction and the remaining lengths of the ZnO NWs. Therefore, the device structures here are likely to operate as a hybrid of both photodiode and photoconductor modes. For both devices D1 and D2, two bands were observed for photoresponsivity spectra under reverse bias condition. The first band is in the UV region (250–375 nm), while the second band located at the visible region (450–800 nm). In contrast, the responsivity in the visible region was in the noise level when forward biased. The voltage polarity dependence of the responsivity spectra is attributed to the high valence band offset in the interfacial region of ZnO and *p*-Si substrate, which block the movement of the photogenerated holes from *p*-Si to ZnO NWs.²⁷

In conclusion, MWCNTs network as electrode was deposited on ZnO NWs/*p*-Si heterojunction photodiode grown by hydrothermal process. Fast transient response with rise time 0.09 s and fall time 0.08 s was observed for the photodiode with MWCNTs network. The photodiode also showed higher responsivity in the UV region (4.7 A/W at 365 nm, 2 V) compared with the reference sample and most of the reported works. The faster transient response and the higher photoresponsivity are attributed to better integrity of the device and reduced series resistance effect by applying the MWCNTs network, which effectively improved carrier collection and transport efficiency. The operation of devices in this work is discussed as a photodiode and photoconductor hybrid, which introduce the high internal gain and therefore

high photoresponsivities. The voltage polarity dependence of the responsivity spectra is due to the high valence band offset in the interfacial region of ZnO and *p*-Si substrate.

The authors gratefully acknowledge support from National Security Technologies through NSF Industry/University Cooperative Research Center Connection One. The authors also acknowledge the National Science Foundation Smart Lighting Engineering Research Center (EEC-0812056) and a NSF career Award DMR 1151028. The author Yu thanks for the financial support from China Scholarship Council (CSC File No.2010646040).

- ¹C.-Y. Chang, F.-C. Tsao, C.-J. Pan, G.-C. Chi, H.-T. Wang, J.-J. Chen, F. Ren, D. P. Norton, S. J. Pearton, K.-H. Chen, and L.-C. Chen, *Appl. Phys. Lett.* **88**, 173503 (2006).
- ²D. C. Look, C. Coskun, B. Claffin, and G. C. Farlow, *Physica B* **340**, 32 (2003).
- ³C. Soci, A. Zhang, B. Xiang, S. A. Dayeh, D. P. R. Aplin, J. Park, X. Y. Bao, Y. H. Lo, and D. Wang, *Nano Lett.* **7**, 1003 (2007).
- ⁴E. Lai, W. Kim, and P. Yang, *Nano Res.* **1**, 123 (2008).
- ⁵S. Chu, G. Wang, W. Zhou, Y. Lin, L. Chernyak, J. Zhao, J. Kong, L. Li, J. Ren, and J. Liu, *Nat. Nanotechnol.* **6**, 506 (2011).
- ⁶L. Wang, X. Zhang, S. Zhao, G. Zhou, Y. Zhou, and J. Qi, *Appl. Phys. Lett.* **86**, 024108 (2005).
- ⁷J. Wang and L. Gao, *Solid State Commun.* **132**, 269 (2004).
- ⁸Z. Y. Fan, D. Dutta, C. J. Chien, H. Y. Chen, and E. C. Brown, *Appl. Phys. Lett.* **89**, 213110 (2006).
- ⁹S.-W. Kim, S. Fujita, and S. Fujita, *Appl. Phys. Lett.* **86**, 153119 (2005).
- ¹⁰C. H. Bae, S. M. Park, S. E. Ahn, D. J. Oh, G. T. Kim, and J. S. Ha, *Appl. Surf. Sci.* **253**, 1758 (2006).
- ¹¹J. B. Fedison, T. P. Chow, H. Lu, and I. B. Bhat, *Appl. Phys. Lett.* **72**, 2841 (1998).
- ¹²R. Ghosh and D. Basak, *Appl. Phys. Lett.* **90**, 243106 (2007).
- ¹³S. E. Ahn, J. S. Lee, H. Kim, S. Kim, B. H. Kang, K. H. Kim, and G. T. Kim, *Appl. Phys. Lett.* **84**, 5022 (2004).
- ¹⁴L. J. Brillson and Y. Lu, *J. Appl. Phys.* **109**, 121301 (2011).
- ¹⁵H. Ago, T. Kugler, F. Cacialli, W. R. Salaneck, M. S. P. Shaffer, A. H. Windle, and R. H. Friend, *J. Phys. Chem. B* **103**, 8116 (1999).
- ¹⁶M. P. Anantram and F. Leonard, *Rep. Prog. Phys.* **69**, 507 (2006).
- ¹⁷I. Robel, B. A. Bunker, and P. V. Kamat, *Adv. Mater.* **17**, 2458 (2005).
- ¹⁸M. Liu and H. K. Kim, *Appl. Phys. Lett.* **84**, 173 (2004).
- ¹⁹K. W. Liu, R. Chen, G. Z. Xing, T. Wu, and H. D. Sun, *Appl. Phys. Lett.* **96**, 023111 (2010).
- ²⁰D. Shao, L. Qin, and S. Sawyer, *Appl. Surf. Sci.* **261**, 123 (2012).
- ²¹L. Qin, C. Shing, S. Sawyer, and P. Dutta, *Opt. Mater.* **33**, 359 (2010).
- ²²L. Luo, Y. Zhang, S. Mao, and L. Lin, *Sens. Actuators, A* **127**, 201 (2006).
- ²³I. S. Jeong, J. H. Kim, and S. Lm, *Appl. Phys. Lett.* **83**, 2946 (2003).
- ²⁴C. H. Park, I. S. Jeong, J. H. Kim, and S. Im, *Appl. Phys. Lett.* **82**, 3973 (2003).
- ²⁵B. Gupta, A. Jain, and R. M. Mehra, *J. Mater. Sci. Technol.* **26**, 223 (2010).
- ²⁶Y. S. Choi, J. Y. Lee, S. Im, and S. J. Lee, *J. Vac. Sci. Technol. B* **20**, 2384 (2002).
- ²⁷H.-D. Um, S. A. Moiz, K.-T. Park, J.-Y. Jung, S.-W. Jee, C. H. Ahn, D. C. Kim, H. K. Cho, D.-W. Kim, and J.-H. Lee, *Appl. Phys. Lett.* **98**, 033102 (2011).
- ²⁸Q. Yang, X. Guo, W. Wang, Y. Zhang, S. Xu, D. H. Lien, and Z. L. Wang, *ACS Nano* **4**, 6285 (2010).